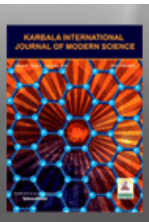

Karbala International Journal of Modern Science

Volume 6 | Issue 3 Article 8

Dynamic Analysis of Viscoelastic Circular Diaphragm of a MEMS Capacitive Pressure Sensor using Modified Differential Transformation Method

Dr Olurotimi A. Adeleye
University of Lagos, Nigeria, rotimiadeleye1711@gmail.com

Muritala Yusuf
University of Lagos, Nigeria, muritalayusuf11@gmail.com

Oluwaseyi .. Balogun
University of Lagos, Akoka, Lagos, 3jbalogun@unilag.edu.ng

Dynamic Analysis of Viscoelastic Circular Diaphragm of a MEMS Capacitive Pressure Sensor using Modified Differential Transformation Method

Abstract

In this paper, a dynamic analysis of the viscoelastic circular diaphragm of a Micro-Electro-Mechanical System (MEMS) capacitive pressure sensor using the Modified Differential Transformation Method (MDTM) is presented. The MEMS technology has been increasingly used to fabricate sensors and actuators and the MEMS capacitive pressure sensor is emerging in many high-performance applications. The deflection of these sensors diaphragm (plate) depends largely on the material of the diaphragm. In this study, a circular diaphragm of viscoelastic material is modeled using the classical plate theory. The governing differential equation is solved using Modified Differential Transformation Method (MDTM) and the result is validated with Finite Difference Method (FDM). The result shows excellent agreement with the numerical method. The effects of amplitudes, frequency, viscoelastic parameter, and time of applied pressure on deflection of the viscoelastic circular diaphragm are investigated. It is established from the results that the deflection of the sensor increases with an increase in the amplitude, frequency and time of the applied pressure. In addition, an increase in the viscoelastic parameters resulted in an increase the deflection of the diaphragm which consequently increases the capacitance and sensitivity of the sensor. Hence, the viscoelastic circular diaphragm of the MEMS capacitive pressure sensor exhibits better sensitivity performance when compared with that of elastic material. Finally, the Modified Differential Transformation Method applied in obtaining the solution of the developed model is effective in predicting sensor characteristics. The study will enhance the design of MEMS capacitive pressure sensor with viscoelastic circular diaphragm.

Keywords

Dynamic analysis; MEMS Capacitive pressure sensor; Viscoelasticity; Circular diaphragm; Differential Transformation Method; Padé approximant

Cover Page Footnote

MDTM - Modified Differential Transformation Method, MEMS - Micro-Electro-Mechanical System

ACKNOWLEDGMENTS Though no extra fund was needed for this study, we acknowledge the provision of computer systems for simulation of results by Energy Research Laboratory, Faculty of Engineering, University of Lagos.

1. Introduction

The various applications of MEMS technology in engineering processes have continued to attract research interests in the production of miniaturized devices with mechanical functionality, automotive industry and other areas of engineering applications. These applications include; production of pressure sensors, accelerometer sensors, ink jet printers, disposable blood pressure meters, and engine oil pressure sensors, evaporative purge system leak detection, tire pressure, air-bag system, brake system and the utility systems that control the vehicle body functions in automotive industry [1−3]. These applications are also increasing because of the functionality and versatility of the products, which exhibit great advantages over the previous one. The new MEMS pressure sensor for instance has low weight, small size, smart function, and it is highly reliable and affordable [4−6]. The functionality of the MEMS capacitive pressure sensor has been enhanced with the smart functions and this has increased its performance over piezo-resistive pressure sensor [5,6]. Some of the performance indices include high sensitivity, circuitry compatibility, low power consumption rate, low noise, low thermal sensitivity and large dynamic range. Remarkably, these performance functions, reliability features and the production method of the MEMS pressure sensor are achieved at low cost [1].

The behavior of MEMS capacity pressure sensor with different material properties has been modeled. In the modeling approach, the deflection of the sensor diaphragm depends on factors such as geometry, the type of loading on the diaphragm and type of material of the diaphragm. The geometry of the diaphragm includes rectangular, square or circular cross-section, and thin or thick size. It is observed that rectangular diaphragm exhibited higher stress than square and circular diaphragms. The second factor is the type of loading on the diaphragm which includes gradually applied or impact loading and the point of application of the load on the upper moving plate (while the bottom is stationary) [7,8]. The gradually applied loading or the touch mode model has been developed [9]. The third factor which has a major role to play in the developed model of the diaphragm is the type of material of the diaphragm. Various materials and material models including elastic materials have been used in past applications and modeling approach of MEMS capacitor sensor diaphragm [1]. But in recent studies, silicon and other polymeric materials have been used for the diaphragm. These materials are fast replacing the traditional metal diaphragm used in the capacitance pressure sensors [2−4,10−12]. They are widely used because of their economic values, their availability, versatility and affordability. Other advantages of this polymeric material include structural stability, flexibility and good electrical and thermal characteristics. Silicon carbide (SiC) has been used for circular diaphragm because of its high temperature applications which can be up to about 400 °C and pressure range of 0−333 kPa [2,3,10]. Remarkably, polysilicon with various configurations is widely used as a diaphragm material [1,5]. Polyimide materials possess an exceptionally good balance of chemical, electrical, and physical properties for a large temperature range. Their dimensions are stable at high temperatures and they have excellent adhesion properties [4]. But, these time and path dependent viscoelastic material properties have not been adequately captured in the existing models of the MEMS capacity pressure sensor of circular diaphragm.

Therefore, in the present study, the MEMS capacity pressure sensor of circular diaphragm with viscoelastic material is modeled using the classical plate theory and the governing equation is solved by applying the Modified Differential Transformation Method (MDTM). The Modified Differential Transformation Method is a hybrid of the conventional Differential Transform, Inverse transform, Laplace transform, and Padé approximation methods. The Differential Transform Method (DTM) is a semi-analytical method for solving linear and strongly non-linear differential equations particularly of higher orders. It was developed by J. K. Zhou and tends to be less intensive in terms of computational analysis when compared to HPM [13]. The DTM has proven to be very effective in comparison with other approximate analytical solutions as it requires fewer computations as done with Adomian decomposition method (ADM), homotopy perturbation method (HPM), homotopy analysis method (HAM), and variational iteration method (VIM). Remarkably, the requirements of small perturbation parameter of the traditional Perturbation Methods, the rigorous technique applied in obtaining Adomian polynomials as done in ADM, the inefficiency of obtaining solutions to weakly nonlinear differential equations by HPM, the unavailability of

https://doi.org/10.33640/2405-609X.1706

proper theories for determining initial approximation, and auxiliary functions, parameters, linear operators, and the conformity requirements of the obtained solution to the coefficient periodicity rule as required in HAM, the search for Langrange multiplier also required in VIM, and the difficulties with determining the approximate functions for the geometry of interest as carried out in collocation method (CM), least square method (LSM), and Galerkin weighted residual method (GWRM), are few of the challenges that have been overcome with DTM.

The DTM is more accurate than the Generalized Differential Method [14], and its characteristics have been highlighted [15]. The efficiency of the DTM has been combined with other methods [16] to obtain better results. The DTM techniques have been applied in the study Biomaterials [17], to obtain creep strain relaxation behavior of these materials. But the DTM has some shortcomings; in that the series solution has slowed convergent rate and may oscillate. In order to overcome these drawbacks, the Modified Differential Transform Method was developed to solve differential equations. In the MDTM solution procedure, the Padé approximant of DTM solution is treated with Laplace and inverse Laplace transforms. The Padé approximation is used to increase the convergence rate and the stability of the truncated series solution obtained from DTM. Thus, solutions of MDTM are always valid and stable [18,19]. The Padé approximation method used in MDTM serves as an after-treatment technique to correct the shortcoming of the solution obtained from DTM. Padé approximation method is often used to express a series solution (polynomial) in rational form so as to extend the domain of convergence of the independent variable. Remarkably, the transformation of a model solution to Padé form increases rate of convergence and provides good approximations even beyond the radius of convergence of the power series expansion [18].

Hence the main objective of this study is to develop a dynamic analysis of the viscoelastic circular diaphragm of a Micro-Electro-Mechanical System (MEMS) capacitive pressure sensor using the Modified Differential Transformation Method. The obtained result is validated with Finite Difference Method (FDM) and the effects of amplitudes, frequency, viscoelastic parameter, and time of applied pressure on deflection of the viscoelastic circular diaphragm are then investigated.

2. Problem formulation

Consider a viscoelastic circular diaphragm of radius r, thickness h and separation between the plates d, of a MEMS capacitive pressure sensor. The parallel plates are clamped at both ends and a pressure $P_0 \cos \omega_s t$is applied which is time dependent as shown in (Fig. 1).

First, the bending analysis of thin plates is considered using the following Kirchhoff's assumptions of classical plate theory [20,21].

I. The plate is assumed to be flat initially.
II. The plate is of viscoelastic material
III. The thickness of the plate is comparatively small to its length and width.
IV. The deflection of the plate is comparatively small to its thickness.
V. The normal straight line to the middle plane before deformation remains so during bending.
VI. The normal stress to the middle plane is comparatively small to other stress components and hence, negligible in the stress–strain relationship.

From the classical theory of plates, Timoshenko [20] stated that the governing differential for the deflection (w) of thin rectangular plates, based on the above Kirchhoff's assumptions, is given by:

$$\frac{\partial^4 w}{\partial x^4}+\frac{\partial^4 w}{\partial y^4}+2\frac{\partial^4 w}{\partial x^2 \partial y^2}=\frac{P}{D} \tag{1}$$

where P = Pressure applied on plate.
D = Flexural rigidity of plate.

Applying the appropriate coordinate transformation technique between Cartesian and polar coordinates, the deflection (w) as a function of $\varphi$and r, is obtained

$$\frac{\partial w}{\partial x}=\frac{\partial w}{\partial r}.\frac{\partial r}{\partial x}+\frac{\partial w}{\partial \varphi}.\frac{\partial \varphi}{\partial x} \tag{2}$$

And

$$\nabla_r^2 w \equiv \frac{\partial^2 w}{\partial x^2}+\frac{\partial^2 w}{\partial y^2}=\frac{\partial^2 w}{\partial r^2}+\frac{1}{r}\frac{\partial w}{\partial r}+\frac{1}{r^2}\frac{\partial^2 w}{\partial \varphi^2} \tag{3}$$

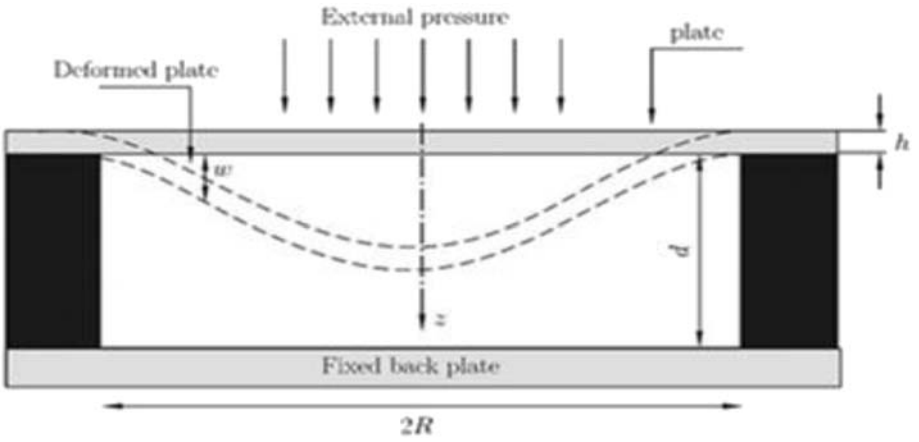

Fig. 1. The sectional diagram of a MEMS capacitive pressure sensor with clamped circular plates.

Substituting Eq. (3) into Eq. (1), the governing equation for circular plate becomes;

$$\frac{\partial^4 w}{\partial r^4}-\frac{1}{r^2}\frac{\partial^2 w}{\partial r^2}+\frac{2}{r}\frac{\partial^3 w}{\partial r^3}+\frac{2}{r^2}\frac{\partial^4 w}{\partial r^2\partial\varphi^2}-\frac{2}{r^3}\frac{\partial^3 w}{\partial r\partial\varphi^2}$$

$$+\frac{4}{r^4}\frac{\partial^2 w}{\partial\varphi^2}+\frac{1}{r^3}\frac{\partial w}{\partial r}+\frac{1}{r^4}\frac{\partial^4 w}{\partial\varphi^4}=\frac{P}{D} \tag{4}$$

Eq. (4) is the governing differential equation for circular plate deflection, which may be rewritten as:

$$D\left(\frac{\partial^4 w}{\partial r^4}-\frac{1}{r^2}\frac{\partial^2 w}{\partial r^2}+\frac{2}{r}\frac{\partial^3 w}{\partial r^3}+\frac{1}{r^3}\frac{\partial w}{\partial r}+\frac{1}{r^4}\frac{\partial^4 w}{\partial\varphi^4}+\frac{2}{r^2}\frac{\partial^4 w}{\partial r^2\partial\varphi^2}+\frac{4}{r^4}\frac{\partial^2 w}{\partial\varphi^2}-\frac{2}{r^3}\frac{\partial^3 w}{\partial r\partial\varphi^2}\right)=P \tag{5}$$

2.1. Axisymmetric bending of circular plate of viscoelastic material

When the end restraints and applied pressure of a circular plate do not depend on φsuch that the plate deflection and stress resultants (and couples) depend on $r$only, then the bending of the circular plate is described as being axially symmetrical or simply axisymmetric.

Thus, for axisymmetric bending analysis of circular plates, Eq. (5) reduces to:

$$D\left(\frac{\partial^4 w}{\partial r^4}+\frac{2}{r}\frac{\partial^3 w}{\partial r^3}-\frac{1}{r^2}\frac{\partial^2 w}{\partial r^2}+\frac{1}{r^3}\frac{\partial w}{\partial r}\right)=P \tag{6}$$

Also, from Fig. 1, the MEMS sensor is assumed to work in normal mode, where the deflection of the plate is comparatively small to the diaphragm thickness, then the relationship between the displacement w of the diaphragm to the applied pressure P is given by:

$$P=\rho h\frac{\partial^2 w}{\partial t^2} \tag{7}$$

where ρ = plate density.

Finally, upper plate (diaphragm) is made of a viscoelastic material, using the Maxwell's model of a viscoelastic material; the total stress (pressure) on the viscoelastic plate is given as:

$$\sigma=\kappa w+\eta\frac{\partial w}{\partial t} \tag{8}$$

where κ = plate stiffness.

η = plate viscosity.

Based on the assumptions above and summing Eqs. (6)–(8), the overall pressure on the upper plate of the MEMS sensor is expressed as:

$$D\left(\frac{\partial^4 w}{\partial r^4}+\frac{2}{r}\frac{\partial^3 w}{\partial r^3}-\frac{1}{r^2}\frac{\partial^2 w}{\partial r^2}+\frac{1}{r^3}\frac{\partial w}{\partial r}\right)+T\left(\frac{\partial^2 w}{\partial r^2}+\frac{1}{r}\frac{\partial w}{\partial r}\right)+\rho h\frac{\partial^2 w}{\partial t^2}+\kappa w+\eta\frac{\partial w}{\partial t}=P_0\cos(w_s t) \tag{9}$$

Since the diaphragm deflection w depends on radius r and time t, then we can rewrite Eq. (9) as:

$$D\left(\frac{\partial^4}{\partial r^4}+\frac{2}{r}\frac{\partial^3}{\partial r^3}-\frac{1}{r^2}\frac{\partial^2}{\partial r^2}+\frac{1}{r^3}\frac{\partial}{\partial r}\right)w(r,t)+T\left(\frac{\partial^2}{\partial r^2}+\frac{1}{r}\frac{\partial}{\partial r}\right)w(r,t)+\kappa w(r,t)+\rho h\frac{\partial^2 w(r,t)}{\partial t^2}+\eta\frac{\partial w(r,t)}{\partial t}\ =\ P_0\cos(w_s t) \tag{10}$$

The plate has the following initial conditions:

$$w(r,0)=0,\ \dot{w}(r,0)=0 \tag{11}$$

where $\dot{w}$ is. $\frac{dw}{dt}$

Since the circular plate is assumed to be clamped at both ends, the clamped plate has the following boundary conditions:

$$w(b)=0,\ \left.\frac{dw}{dr}\right|_{r=b}=0 \tag{12}$$

Eq. (10) is a fourth -order differential equation, and so requires four boundary conditions in order to determine the solution. Two of them have been obtained as given in Eqs. (11) and (12). Others are obtained from the condition of regularity at the plate center and are expressed as

$$\frac{dw}{dr}=0,\ V_r=\frac{d^3 w}{dr^3}+\frac{1}{r}\frac{d^2 w}{dr^2}-\frac{1}{r^2}\frac{dw}{dr}=0 \text{ at } r=0 \tag{13}$$

3. Method of solution

3.1. Modified Differential Transformation Method (MDTM)

In this section, the Modified Differential Transformation Method (MDTM) and the Finite Difference Method (FDM) are applied to solve the governing differential equation. In the MDTM, the model is first solved by differential transform method. The solution obtained is transformed by Laplace transform into s-domain and the Padé approximant of the resulting solution is obtained. Finally, the inverse Laplace transform is applied to obtain the final solution in time-domain.

By applying two-dimensional DTM, the governing equation (13) above is transformed into an algebraic equation as follows:

$$\begin{aligned}&D\left(\begin{array}{l}(k+4)(k+3)(k+2)(k+1)W(k+4,h)\\ +2\sum_{l=0}^{k}\sum_{p=0}^{h}\delta(l+1,h-p)(k-l+3)(k-l+2)(k-l+1)W(k-l+3,p)\\ -\sum_{l=0}^{k}\sum_{p=0}^{h}\delta(l+2,h-p)(k-l+2)(k-l+1)W(k-l+2,p)\\ +\sum_{l=0}^{k}\sum_{p=0}^{h}\delta(l+3,h-p)(k-l+1)W(k-l+1,p)\end{array}\right)\\ &+T\left((k+1)(k+2)W(k+2,h)+\sum_{l=0}^{k}\sum_{p=0}^{h}\delta(l+1,h-p)(k-l+1)W(k-l+1,p)\right)\\ &+\rho H(h+1)(h+2)W(k,h+2)+\kappa W(k,h)+\eta(h+1)W(k,h+1)\ =\ P_0\left(\frac{w_s^h}{h!}\cos\left(\frac{\pi h}{2}\right)\right)\end{aligned} \tag{14}$$

Recall,

$$\delta(k-m,h-n)=\begin{bmatrix}1 & k=m,h=n\\ 0 & \text{elsewhere}\end{bmatrix} \tag{15}$$

Substituting (15) into (14) we have:

$$\begin{aligned}&D\begin{pmatrix}(k+4)(k+3)(k+2)(k+1)W(k+4,h)+2(k+4)(k+3)(k+2)W(k+4,h)\\ -(k+4)(k+3)W(k+4,h)+(k+4)W(k+4,h)\end{pmatrix}\\ &\quad+T((k+1)(k+2)W(k+2,h)+(k+2)W(k+2,h))+\rho H(h+1)(h+2)W(k,h+2)+\kappa W(k,h)\\ &\quad+\eta(h+1)W(k,h+1)\;=\;P_0\left(\frac{w_s^h}{h!}\cos\left(\frac{\pi h}{2}\right)\right)\end{aligned} \tag{16}$$

Simplifying Eq. (16), the model reduces

$$W(k+4,h)=\frac{1}{D(k+4)^2(k+2)^2}\begin{pmatrix}P_0\left(\frac{w_s{}^h}{h!}\cos\left(\frac{\pi h}{2}\right)\right)-\kappa W(k,h)-T(k+2)^2W(k+2,h)\\ -\rho H(h+1)(h+2)W(k,h+2)-\eta(h+1)W(k,h+1)\end{pmatrix} \tag{17}$$

The deflection $W(k,h)$is obtained for
$W(k,0)=0$ for all $k\geq 0...4,\ h\geq 0...2$ (18)

$$W_{4,0}=\frac{-2Ha\rho+P}{64D} \tag{19}$$

$$W_{4,1}=\frac{-6Ha\rho-2a\eta}{64D} \tag{20}$$

$$W_{4,2}=\frac{-1/2Pw_s^2-4Tb-12Ha\rho-\mu a-3a\eta}{64D} \tag{21}$$

$$W_{6,2}=-\frac{1}{576D}\left(\frac{T\left(\frac{1}{2}Pw_s^2-4Tb-12Ha\rho-\mu a-3a\eta\right)}{4D}+\frac{1}{2}Pw_s^2+12\rho Hb+\mu b+3\eta b\right) \tag{27}$$

$$W_{6,3}=-\frac{1}{576D}\left(\frac{T(-20Ha\rho-4Tb-4a\eta-\mu a)}{4D}+20\rho Hb+\mu b+4\eta b\right) \tag{28}$$

$$W_{5,0}=\frac{-2Hc\rho+P}{225D} \tag{22}$$

$$W_{5,1}=\frac{-6Hc\rho-2c\eta}{225D} \tag{23}$$

$$W_{5,2}=\frac{-1/2Pw_s^2-9Td-12Hc\rho-\mu c-3c\eta}{225D} \tag{24}$$

$$W_{6,0}=\frac{1}{576D}\left(P-\frac{T(-2Ha\rho+P)}{4D}-2\rho Hb\right) \tag{25}$$

$$W_{6,1}=-\frac{1}{576D}\left(\frac{T(-6Ha\rho-2a\eta)}{4D}+6\rho Hb+2\eta b\right) \tag{26}$$

$$W_{6,4} = -\frac{1}{576D}\left(\frac{T\left(\frac{1}{24}Pw_s^4 - 4Tb - 30Ha\rho - \mu a - 5a\eta\right)}{4D} + \frac{1}{24}Pw_s^4 + 30\rho Hb + \mu b + 5\eta b\right) \tag{29}$$

The obtained coefficients in Eqs. (19)–(29) are substituted into Eq. (17) to obtain:

$$+T\left(\frac{\partial^2}{\partial r^2}+\frac{1}{r}\frac{\partial}{\partial r}\right)w(r,t)+\rho h\frac{\partial^2}{\partial t^2}w(r,t) +\kappa w(r,t)+\eta\frac{\partial}{\partial t}w(r,t)=P(w_s,t) \tag{31}$$

3.2. Validation of the MDTM result with the finite difference method

$$W[k,h]=dr^3t^3+dr^3t^2+crt^2+at^4+br^2t^3+crt^3+br^2t^2+at^2+crt^4+at^3+br^2t^4-\frac{2\rho Hcr^5}{225D}-\frac{3\rho Har^4t}{32D}-\frac{2Hc\rho r^5}{225D}$$
$$+\frac{(-2\rho Ha+P)r^4}{64D}-\frac{2\rho Hcr^5t}{75D}-\frac{r^6}{576D}\left(\frac{T(-2\rho Ha+P)}{4D}+2\rho Hb\right)+\frac{r^6t^2}{576D}\left(\frac{T(12Ha\rho+4Tb)}{4D}-12\rho Hb\right)$$
$$+\frac{(-12Ha\rho-4Tb)r^4t^2}{64D}+\frac{(-20Ha\rho-4Tb)r^4t^3}{64D}+\frac{(-30Ha\rho-4Tb)r^4t^4}{64D}+\frac{r^6t^3}{576D}\left(\frac{T(20Ha\rho+4Tb)}{4D}-20\rho Hb\right)$$
$$+\frac{(-20Hc\rho-9Td)r^5t^3}{225D}+\frac{(-30Hc\rho-9Td)r^5t^4}{225D}+\frac{r^6t}{576D}\left(\frac{3T}{2}\frac{\rho Ha}{D}-6\rho Hb\right)+\frac{(-12Hc\rho-9Td)r^5t^2}{225D}$$
$$+\frac{(-20Hc\rho-9Td)r^5t^3}{225D}+\frac{(-30Hc\rho-9Td)r^5t^4}{225D}+\frac{r^6t^4}{576D}\left(\frac{T(30Ha\rho+4Tb)}{4D}-30Ha\rho\right) \tag{30}$$

Considering the governing differential equation (30),

$$D\left(\frac{\partial^4}{\partial r^4}+\frac{2}{r}\frac{\partial^3}{\partial r^3}-\frac{1}{r^2}\frac{\partial^2}{\partial r^2}+\frac{1}{r^3}\frac{\partial}{\partial r}\right)w(r,t)$$

Applying forward differencing discretization to the governing equation above, we have:

$$D\left(\frac{w_{i+4,j}-4w_{i+3,j}+6w_{i+2,j}-4w_{i+1,j}+w_{i,j}}{(\Delta r)^4}\right)+\frac{2D}{i\Delta r}\left(\frac{w_{i+3,j}-3w_{i+2,j}+3w_{i+1,j}-w_{i,j}}{(\Delta r)^3}\right)-\frac{D}{(i\Delta r)^2}\left(\frac{w_{i+2,j}-2w_{i+1,j}+w_{i,j}}{(\Delta r)^2}\right)$$
$$+\frac{D}{(i\Delta r)^3}\left(\frac{w_{i+1,j}-w_{i,j}}{\Delta r}\right)+T\left(\frac{w_{i+2,j}-2w_{i+1,j}+w_{i,j}}{(\Delta r)^2}\right)+\frac{T}{i\Delta r}\left(\frac{w_{i+1,j}-w_{i,j}}{\Delta r}\right)+\rho H\left(\frac{w_{i,j+2}-2w_{i,j+1}+w_{i,j}}{(\Delta t)^2}\right)+\kappa w_{i,j}$$
$$+\eta\left(\frac{w_{i,j+1}-w_{i,j}}{\Delta t}\right)=P \tag{32}$$

Multiplying through by $(\Delta t)^2(i\Delta r)^4$ and taking $\Delta r = h$ and $\Delta t = k$, we have:

By simplification,

$$Dk^2i^4\left(w_{i+4,j}-4w_{i+3,j}+6w_{i+2,j}-4w_{i+1,j}+w_{i,j}\right)+2Dk^2i^3\left(w_{i+3,j}-3w_{i+2,j}+3w_{i+1,j}-w_{i,j}\right)-$$
$$Dk^2i^2\left(w_{i+2,j}-2w_{i+1,j}+w_{i,j}\right)+Dk^2i\left(w_{i+1,j}-w_{i,j}\right)+Th^2k^2i^4\left(w_{i+2,j}-2w_{i+1,j}+w_{i,j}\right)+ \quad (33)$$
$$Th^2k^2i^3\left(w_{i+1,j}-w_{i,j}\right)+\rho Hh^4i^4\left(w_{i,j+2}-2w_{i,j+1}+w_{i,j}\right)+Kh^4k^2i^4w_{i,j}+$$
$$\eta h^4ki^4\left(w_{i,j+1}-w_{i,j}\right)=(P_0\cos\omega_s(ik))h^4k^2i^4$$

$$\left(Dk^2i^4\right)w_{i+4,j}+\left(-4Dk^2i^4+2Dk^2i^3\right)w_{i+3,j}+\left(6Dk^2i^4-6Dk^2i^3-Dk^2i^2+Th^2k^2i^4\right)w_{i+2,j}+$$
$$\left(-4Dk^2i^4+6Dk^2i^3+2Dk^2i^2+Dk^2i-2Th^2k^2i^4+Th^2k^2i^3\right)w_{i+1,j}+\left(Dk^2i^4-2Dk^2i^3-Dk^2i^2-Dk^2i+Th^2k^2i^4\right.$$
$$\left.-Th^2k^2i^3+\rho Hh^4i^4+Kh^4k^2i^4-\eta h^4ki^4\right)w_{i,j}+\left(\rho Hh^4i^4\right)w_{i,j+2}+\left(-2\rho Hh^4i^4+\eta h^4ki^4\right)w_{i,j+1}$$
$$=(P_0\cos\omega_s(ik))h^4k^2i^4 \quad (34)$$

Now, the initial and boundary conditions are also discretized using FDM by central differencing. Thus, we have:

$w_{i,0} = 0,\ w_{i,j+1} = w_{i,j-1}$ at j = 0

$w_{1,j}=0, w_{2,j}=w_{0,j}$ at i = 1

$w_{1+1,j}=w_{1-1,j},\ w_{1+2,j}=w_{1-2,j}\ at\ i = 0$

Substituting the transformed boundary conditions above into Equation (34) on MAPLE application, the generated result is shown in Table 1.

4. Result and discusion

The results from the MDTM simulations of the solution model for the problem investigated and the effects of various parameters on the developed model are presented and discussed. The diaphragm deflection is controlled by the viscoelastic parameters, amplitude, frequency and time of the applied pressure (dynamic load) [1,22]. Also, numerical solution is obtained by Finite Difference Method. The numerical results are compared with the MDTM results to verify the accuracy of the present MDTM computations and presented in (Table 1) and (Fig. 2) Fig. 2. It can be inferred from Table 1 that there is excellent agreement between the MDTM and FDM results.

The diagram of (Fig. 3) shows the variation of plate deflection with dynamic load i.e. diaphragm central deflection for different values of pressure loads. The figure shows that for a given diaphragm radius r, as the amplitude of the pressure increases, the central deflection of the diaphragm also increases [1,12,22]. Also, there is a decrease in the diaphragm deflection as the pressure decreases [20].

The effects of the frequency and amplitude of the dynamic load on the deflection of the diaphragm under study are shown in (Fig. 4) and (Fig. 5) respectively. A thorough study of the two figures helps in understanding the effects of these two important parameters on the stability of the sensor diaphragm (Fig. 4). Indicates that an increase in dynamic pressure frequency leads to a corresponding increase in the number of oscillations of the diaphragm dynamic response which in turn decreases the stability of the sensor diaphragm under study. This is due to an increase in the cycles covered by the diaphragm dynamic response for the same length [22]. While it is shown in (Fig. 5) that an increase in pressure amplitude increases the stability of the diaphragm subjected to the pressure. The reason is that an increase in the dynamic pressure amplitude implies an increase in the magnitude of the pressure acting on the diaphragm.

In (Fig. 6) and (Fig. 7), the dynamic behaviors of the diaphragm of MEMS capacitive pressure sensor subjected to a time-varying pressure are shown. From the results, it is observed that as time is being extended gradually to infinity, the deflection of the diaphragm

Table 1
Table of comparison of results.

R	MDTM (μm)	NUM (FDM) (μm)	Error of MDTM
0.00	0.0000000	0.0000000	0.0000000
0.10	0.0006342	0.0006342	0.0000000
0.20	0.0020043	0.0020042	0.0000001
0.30	0.0034527	0.0034526	0.0000001
0.40	0.0045097	0.0045095	0.0000002
0.50	0.0048933	0.0048932	0.0000002
0.60	0.0045097	0.0045095	0.0000002
0.70	0.0034527	0.0034526	0.0000001
0.80	0.0020043	0.0020042	0.0000001
0.90	0.0006342	0.0006342	0.0000000
1.00	0.0000000	0.0000000	0.0000000

The results of MDTM and Numerical method (FDM) for deflection w (r, t) For ($T = 0.01$N/m, $P = 10$Nm^{-2},$H = 0.005$ mm, $D = 14011.5$ (Nm), $\rho = 2100$ Kgm^{-3}, $w_5 = 500$ rad/s, $\kappa = 0.5$ MNm^{-2},$\eta = 25$ KNsm^{-2}).

increases and vice-versa. The significance of this dynamic analysis is that it helps in the quick monitoring and adjustment of the diaphragm during application [22].

The Dynamic behavior of sensor diaphragm oscillation with time is shown in (Fig. 8), it is observed that the oscillation rises with an increase in time. This is also visible in (Fig. 7). The central deflection of the sensor diaphragm for elastic and viscoelastic material parameters is shown in (Fig. 9).

It is observed from the graph that the deflection of the diaphragm is higher for a (MEMS) capacitive pressure sensor made of a viscoelastic material than the one made of elastic material subjected to the same pressure load. It should be noted that an increase in diaphragm deflection implies an increase in capacitance and sensitivity of the sensor [1,12].

5. Conclusion

In this paper, the dynamic analysis of the viscoelastic circular diaphragm of a Micro-Electro-Mechanical System (MEMS) capacitive pressure sensor using the Modified Differential Transformation Method has been presented. The circular diaphragm of viscoelastic material was modeled using the classical plate theory and the resulting governing differential equation was solved using Modified Differential Transformation Method (MDTM). The obtained result was validated with Finite Difference Method (FDM) and excellent agreement was established between both results. The effects of amplitudes, frequency, viscoelastic parameter, and time of

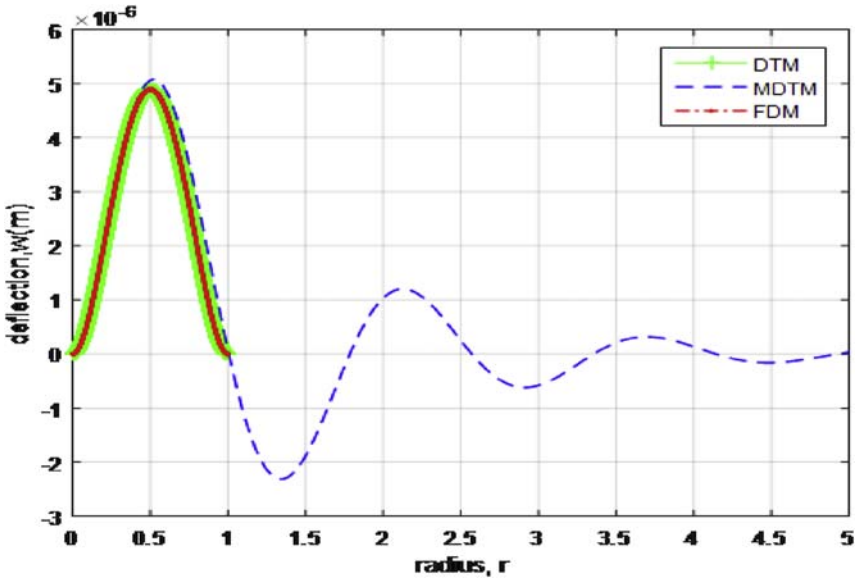

Fig. 2. Comparison of DTM, MDTM and FDM results.

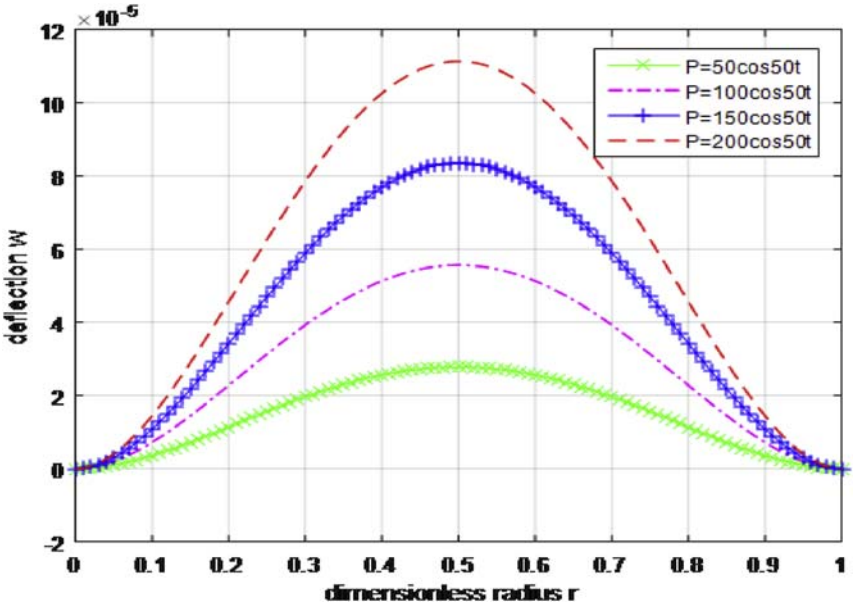

Fig. 3. Effect of pressure change on Deflection.

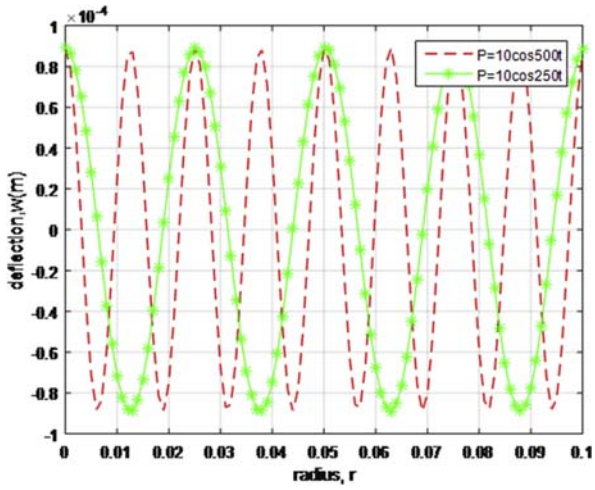

Fig. 4. Variation of plate deflection with pressure frequency.

applied pressure on deflection of the viscoelastic circular diaphragm have been investigated. It is established from the results that the deflection of the sensor increases with an increase in the amplitude, frequency and time of the applied pressure. In addition, an increase in the viscoelastic parameters resulted in an increase the deflection of the diaphragm which consequently increases the capacitance and sensitivity of the sensor. Hence, the viscoelastic circular diaphragm of the MEMS capacitive pressure sensor exhibits better sensitivity performance when compared with that of elastic material. Finally, the method applied in obtaining the solution of the developed model, Modified Differential Transformation Method is effective in predicting sensor characteristics. The study will enhance the design of (MEMS) capacitive pressure sensor with viscoelastic circular diaphragm.

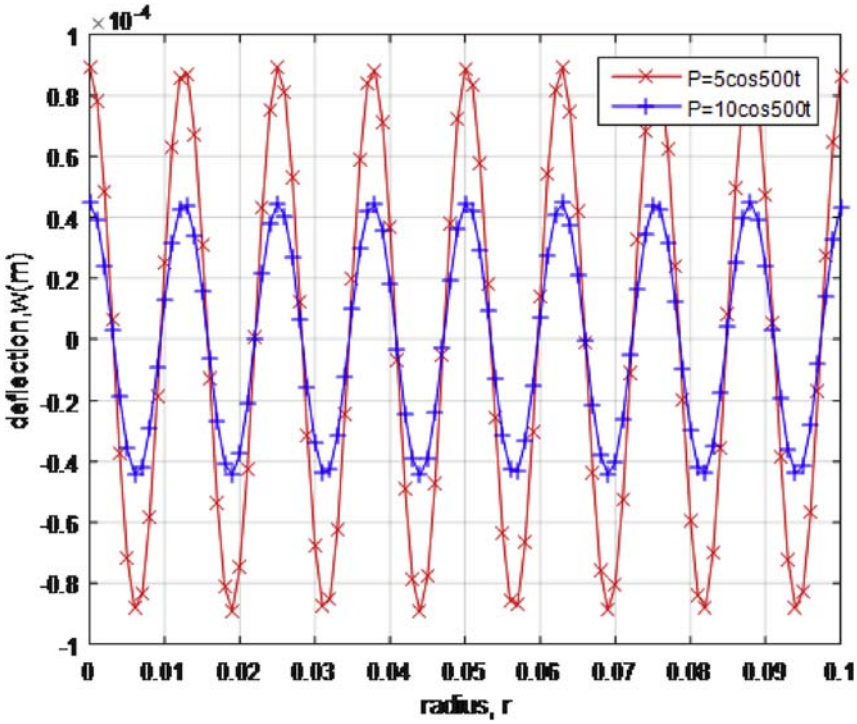

Fig. 5. Variation of deflection with pressure amplitude.

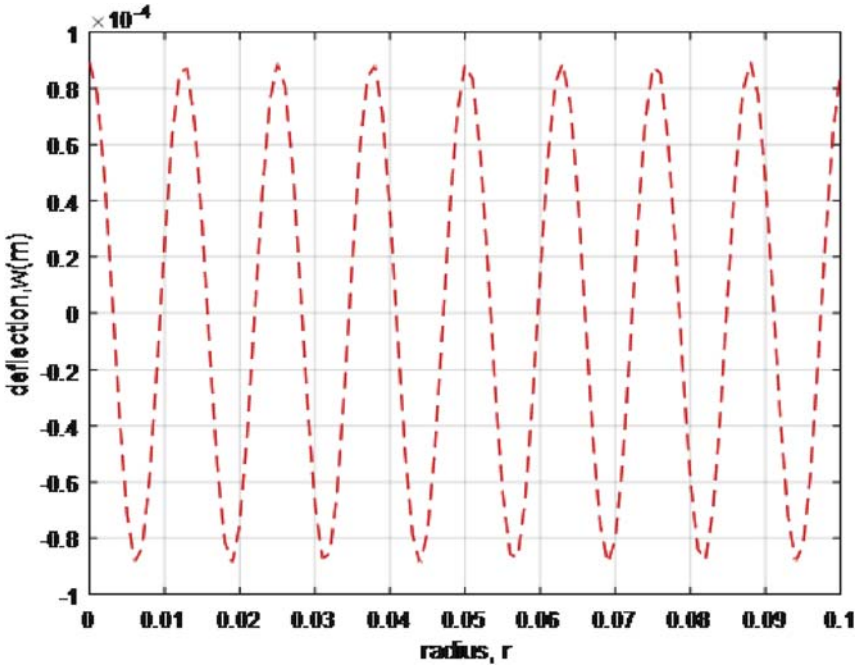

Fig. 6. Dynamic behavior of sensor diaphragm with time t = 0 to t = 0.1.

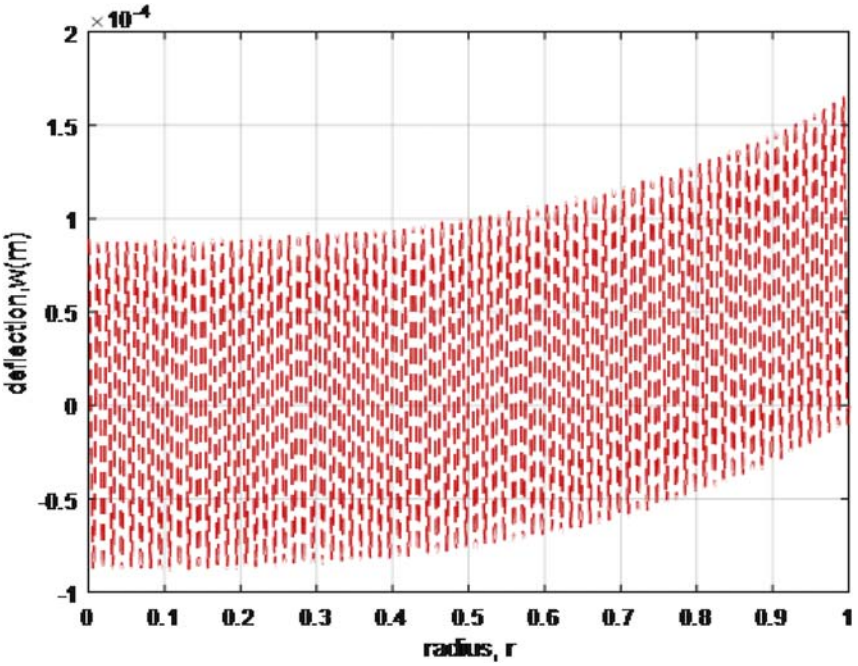

Fig. 7. Dynamic behavior of sensor diaphragm with time t = 0 to t = 1.

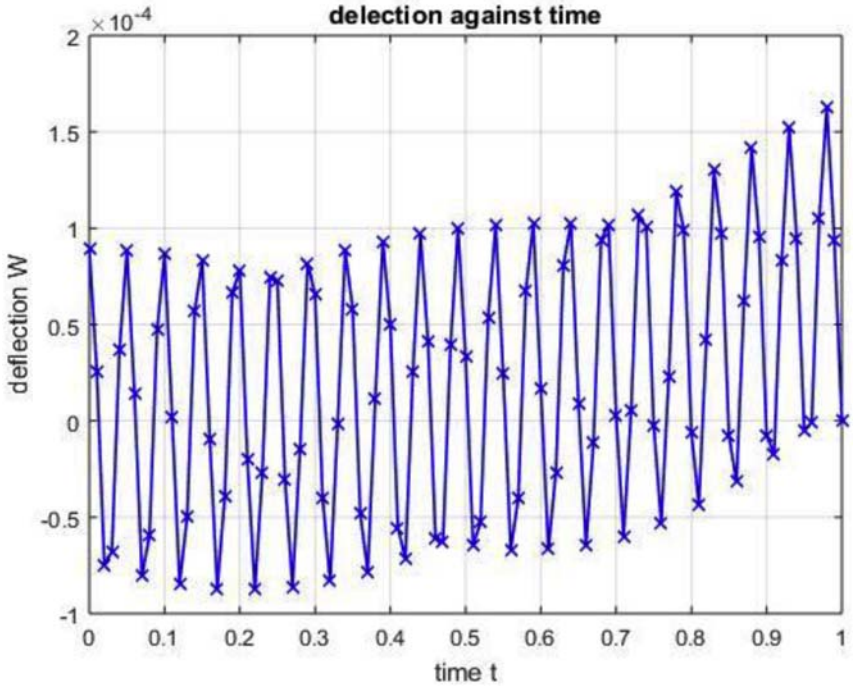

Fig. 8. Dynamic behavior of sensor diaphragm oscillation with time.

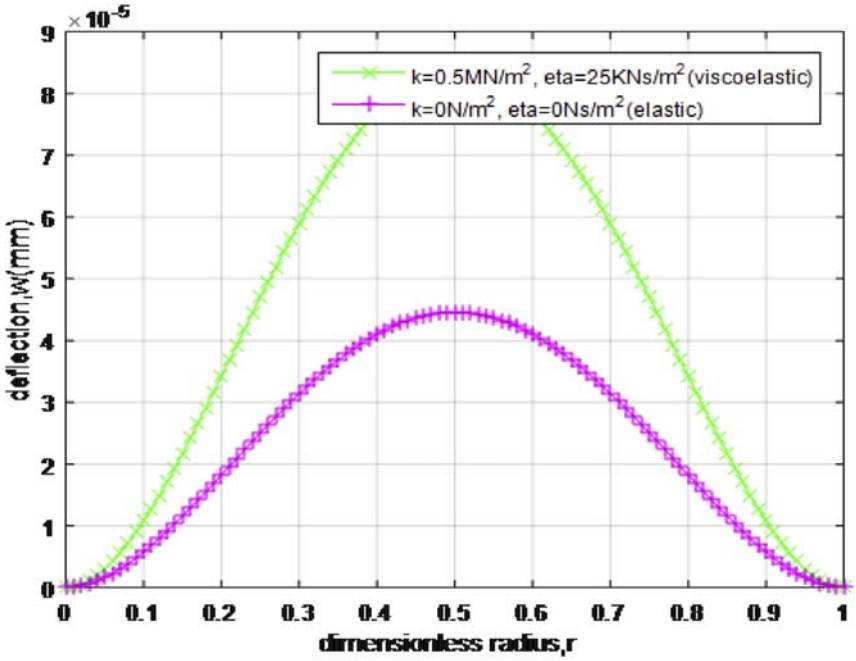

Fig. 9. Deflection of diaphragm against radius for different materials under the same pressure.

Funding source

This research did not receive any specific grant from funding agencies in the public, commercial, or not-for-profit sectors.

Availability of data and material

The datasets used and/or analyzed during the current study are available from the corresponding author on reasonable request.

Declaration of Competing Interest

The authors declare that they have no competing interests.

Acknowledgments

Though no extra fund was needed for this study, we acknowledge the provision of computer systems for simulation of results by Energy Research Laboratory, Faculty of Engineering, University of Lagos.

Nomenclature

D	Flexural rigidity of diaphragm
T	Initial tension per unit length of diaphragm
W	Deflection of plate
r	Radius of plate
h	Thickness of plate
t	Time
E	Young's modulus of diaphragm
P	Applied pressure on plate

Greek letters

τ	Time relaxation of diaphragm
ρ	Density of diaphragm
υ	Poisson ratio of diaphragm
ω_s	Frequency of applied pressure
κ	Stiffness of diaphragm
η	Viscosity of diaphragm
ϵ	Strain

References

[1] M. Molla-Alipour, B.A. Ganji, Analytical analysis of mems capacitive pressure sensor with circular diaphragm under dynamic load using differential transformation method (DTM), Acta Mech. Solida Sin. 28 (4) (2015) 400−408.

[2] N. Marsi, B.Y. Majlis, A.A. Hamzah, F. Mohd-Yasin, The mechanical and electrical effects of MEMS capacitive pressure sensor based 3C-SiC for extreme temperature, J. Eng. (2014) 1−8.

[3] N. Marsi, B.Y. Majlis, F. Mohd-Yasin, A.A. Hamzah, The capacitance and temperature effects of the SiC- and Si-based MEMS pressure sensor, J. Phys. Conf. 431 (1) (2013) 1−9, 012022.

[4] E. Parthasarathy, S. Malarvizhi, Modeling analysis and fabrication of MEMS capacitive differential pressure sensor for altimeter application, J. Chin. Inst. Eng. 41 (3) (2018) 206−215.

[5] Y. Zhang, R. Howver, B. Gogoi, N. Yazdi, A high-sensitive ultra-thin MEMS capacitive pressure sensor, in: 16th International Solid-State Sensors, Actuators, and Microsystems Conference, 2011.

[6] M. Damghanian, B.Y. Majlis, Novel design and fabrication of high sensitivity MEMS capacitive sensor array for fingerprint imaging, Adv. Mater. Res. 74 (2009) 239−242.

[7] A.E. Kubba, A. Hasson, A.I. Kubba, G. Hall, A micro-capacitive pressure sensor design and modelling, J. Sens. Syst. 5 (1) (2016) 95−112.

[8] M.S. Tabarestania, B.A. Ganji, Analytical analysis of capacitive pressure sensor with clamped diaphragm (RESEARCH NOTE), Int. J. Eng. 26 (3) (2013) 297−302.

[9] S.K. Jindal, S.K. Raghuwanshi, Modelling of simply supported circular diaphragm for touch mode capacitive sensors, J. Theor. Appl. Mech. 53 (2) (2015) 431−438.

[10] Y. Hezarjaribi, M.N. Hamidon, S.H. Keshmiri, A.R. Bahadorimehr, Capacitive pressure sensors based on MEMS, operating in harsh environments, IEEE International Conference on Semiconductor Electronics (2008) 184−187.

[11] H.Y. Ma, Q.A. Huang, M. Qin, T. Lu, A micromachined silicon capacitive temperature sensor for radiosonde applications. SENSORS, IEEE., 2009, pp. 1693−1696.

[12] S.P. Chang, M.G. Allen, Capacitive pressure sensors with stainless steel diaphragm and substrate, J. Micromech. Microeng. 14 (4) (2004) 612−618.

[13] J.K. Zhou, Differential Transform Method and its Applications for Electrical Circuits, Huazhong University Press, Wuhan, China, 1986.

[14] M. Garg, P. Manohar, S.L. Kalla, Generalized differential transform method to space-time fractional telegraph equation, International Journal of Differential Equations 2011 (2011) 1−9.

[15] S. Mukherjee, D. Goswami, B. Roy, Solution of higher-order abel equations by differential transform method, Int. J. Mod. Phys. C 23 (9) (2012) 1250056.

[16] O.O. Agboola, A.A. Opanuga, J.A. Gbadeyan, Solution of third order ordinary differential equations using differential transform method, Global J. Pure Appl. Math. 11 (4) (2015) 2511−2517.

[17] O.A. Adeleye, O. Abdulkareem, A.A. Yinusa, M.G. Sobamowo, Analytical investigations of temperature effects on creep strain relaxation of biomaterials using homotopy perturbation and differential transform methods, J. Comput. Appl. Mech. 14 (1−2) (2019) 5−23.

[18] Z. Liu, Y. Yin, F. Wang, Y. Zhao L. Cai, Study on modified differential transform method for free vibration analysis of uniform Euler-Bernoulli beam, Struct. Eng. Mech. 48 (5) (2013) 697−709.

[19] S. Momani, V.S. Ertürk, Solutions of non-linear oscillators by the modified differential transform method, Comput. Math. Appl. 55 (4) (2008) 833−842.

[20] S. Timoshenko, S. Woinowsky-Krieger, in: second ed.Theory of Plates and Shells, McGraw-Hill Book Company Inc., 1959.

[21] E. Ventsel, T. Krauthammer, E. Carrera, Thin plates and shells: theory, analysis, and applications, Appl. Mech. Rev. 55 (4) (2002) B72−B73.

[22] A. Yinusa, G. Sobamowo, Analysis of dynamic behaviour of a tensioned carbon nanotube in thermal and pressurized environments, Karbala International Journal of Modern Science 5 (1) (2019) 1−13.